

UniBrain: Unify Image Reconstruction and Captioning All in One Diffusion Model from Human Brain Activity

Weijian Mai¹, Zhijun Zhang^{1*}
¹South China University of Technology
 drzhangzhijun@gmail.com *

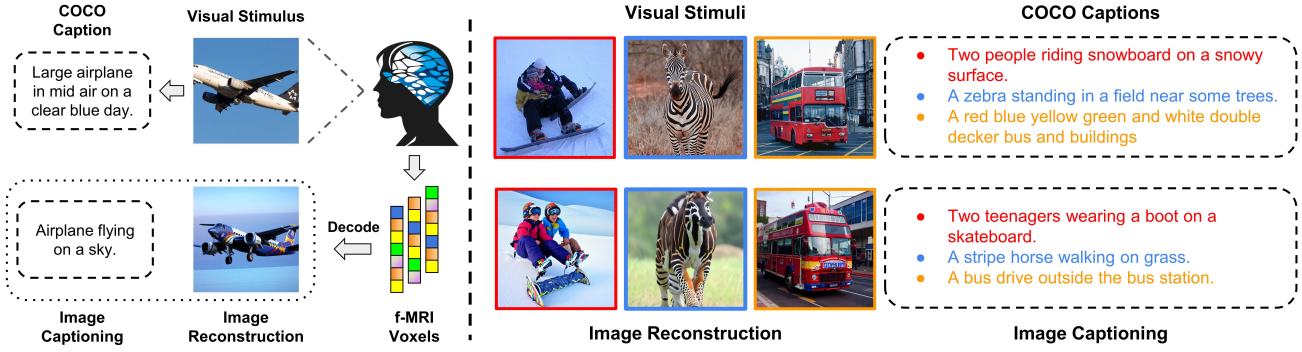


Figure 1. **Brain Decoding for Unified Image Reconstruction and Captioning.** For the first time, our proposed model **UniBrain** decodes fMRI-based brain activities for image reconstruction and captioning all in one diffusion model with both low-level details and high-level semantic fidelity. Left: Multitask overview. Right: More specified image reconstruction and captioning samples. Note that COCO captions are not used as external stimuli to activate fMRI, they are only used as additional training data and raw captions for comparison.

Abstract

Image reconstruction and captioning from brain activity evoked by visual stimuli allow researchers to further understand the connection between the human brain and the visual perception system. While deep generative models have recently been employed in this field, reconstructing realistic captions and images with both low-level details and high semantic fidelity is still a challenging problem. In this work, we propose **UniBrain: Unify Image Reconstruction and Captioning All in One Diffusion Model from Human Brain Activity**. For the first time, we unify image reconstruction and captioning from visual-evoked functional magnetic resonance imaging (fMRI) through a latent diffusion model termed *Versatile Diffusion*. Specifically, we transform fMRI voxels into text and image latent for low-level information and guide the backward diffusion process through fMRI-based image and text conditions derived from CLIP to generate realistic captions and images. UniBrain outperforms current methods both qualitatively and quantitatively in terms of image reconstruction and reports image

captioning results for the first time on the Natural Scenes Dataset (NSD) dataset. Moreover, the ablation experiments and functional region-of-interest (ROI) analysis further exhibit the superiority of UniBrain and provide comprehensive insight for visual-evoked brain decoding.

1. Introduction

How does the human brain process and understand external visual stimuli? Image reconstruction and captioning from brain activity (i.e. functional magnetic resonance imaging (fMRI)) may give us a plausible answer. Image reconstruction from visual-evoked fMRI could potentially be used to create brain-computer interfaces that can decode what someone is seeing or even help individuals with certain neurological conditions communicate their visual experiences. Instead of reconstructing the actual visual image, image captioning from visual-evoked fMRI focuses on generating descriptive captions or textual explanations of the visual stimuli, which could have applications in helping individuals with communication difficulties express their visual experiences or in developing brain-computer interfaces

*Corresponding author

that can translate brain activity into natural language descriptions. Combining image reconstruction and captioning from visual-evoked fMRI would create a powerful system that not only reconstructs the visual image that a participant is viewing but also generates a descriptive caption or textual explanation of that image. This combined approach could provide a more comprehensive understanding of the participant’s visual experience, bridging the gap between neural activity and language comprehension. However, to the best of our knowledge, no previous work has attempted to design a unified framework for deeper and more comprehensive analysis.

Image reconstruction from visual-evoked fMRI is an intriguing yet difficult task due to the limited understanding of potential neural representations and the typically small sample size of neural data. [14] [19] [21]. Researchers have recently begun to focus on image reconstruction tasks by utilizing deep generative models (i.e. generative adversarial networks (GANs)) [17] [8] [32] [20] [10] [25], as well as self-supervised learning [3] [9]. Furthermore, recent research has improved the semantic fidelity by explicitly incorporating semantic content as supplementary information for reconstruction [8] [17]. Nevertheless, these investigations necessitate training from scratch or fine-tuning complex deep generative models using limited neural data. This imbalance between data and parameters limits model performance in terms of pixel and semantic fidelity. Image captioning needs to build connections between multiple modalities of brain data, stimulus images, and semantic text. Contextual associations of text data often need to be captured using sequence models. Hence, current researchers tend to use a hybrid structure of Convolutional Neural Networks (CNN) and sequence models (i.e. Recurrent Neural Networks(RNN), Transformer) to decode visual-evoked fMRI into language step by step [13] [43].

In recent years, diffusion models (DMs) [11] [33] [34] have garnered significant interest as deep generative models. DMs have demonstrated exceptional performance in various tasks, including image colorization [27], image super-resolution [29], conditional image generation [7] [28] [35], and other relevant tasks [22] [30], establishing themselves as the leading models in these areas. As an improvement, latent diffusion models (LDMs) [26] have achieved computational expense reduction through the utilization of the latent space produced by their autoencoding elements. This allows for more efficient calculations during training and inference, as well as the capability to generate high-resolution images with high semantic fidelity. On the one hand, Takagi *et al.* [38] first attempted to map fMRI to the input space of a text-guided latent diffusion model (Stable Diffusion) and generate high-fidelity images without training or fine-tuning deep neural networks. However, the reconstructed images of this model are still not semantic and

natural enough, probably due to the limited single-modality (only text) condition. On the other hand, to the best of our knowledge, no study has used diffusion models for image captioning from visual-evoked fMRI, let alone performing fMRI-based image reconstruction and captioning all in one diffusion model.

To tackle these issues, we propose a multi-task diffusion framework with multi-modality conditions (text and image) termed UniBrain based on Versatile Diffusion (VD) [42] for visual-evoked fMRI-based image reconstruction and captioning. UniBrain is capable of generating images and descriptive captions from human brain activity (fMRI) evoked by visual stimuli (Figure 1). The contributions of this paper are as follows:

- By mapping fMRI to the input space of diffusion, UniBrain is capable of generating high-quality images and captions from fMRI without any training and fine-tuning of the deep learning model.
- UniBrain uses multi-modality conditions (image and text) to guide the generation of images and captions, significantly improving semantic fidelity compared to typical text-guide diffusion models.
- For the first time, a unified model UniBrain is proposed for visual-evoked fMRI-based image reconstruction and captioning. While achieving state-of-the-art on each task, UniBrain also contributes to a more comprehensive analysis of how human brain processes and understands external visual stimuli.

2. Methodology

2.1. Latent Diffusion Models

Diffusion Models (DMs) refer to probabilistic generative models that utilize iterative denoising to recover a sampled variable from Gaussian noise and transform it into a sample conforming to the learned data distribution. The gradual incorporation of Gaussian noise through the forward diffusion process disrupts the inherent structure of the raw training data. The noisy variant of the initial input x_0 at each time point is defined as $x_t = \sqrt{\alpha_t}x_0 + \sqrt{1 - \alpha_t}\epsilon_t$. The reverse diffusion process is learned via a neural network (Denoising U-Net) to predict and remove noise from the noisy input so as to retrieve the original variables. This is done by minimizing the loss function as follows:

$$L_{DM} = E_{x_0, \epsilon \sim \mathcal{N}(0,1), t} [\|\epsilon - \epsilon_\theta(x_t, t)\|^2] \quad (1)$$

where α represents the control factor for adding noise, ϵ is the true Gaussian noise, $\epsilon_\theta(\cdot)$ represents the neural network trained to predict the noise, and $t \in \{1, 2, \dots, T\}$ denotes the time step.

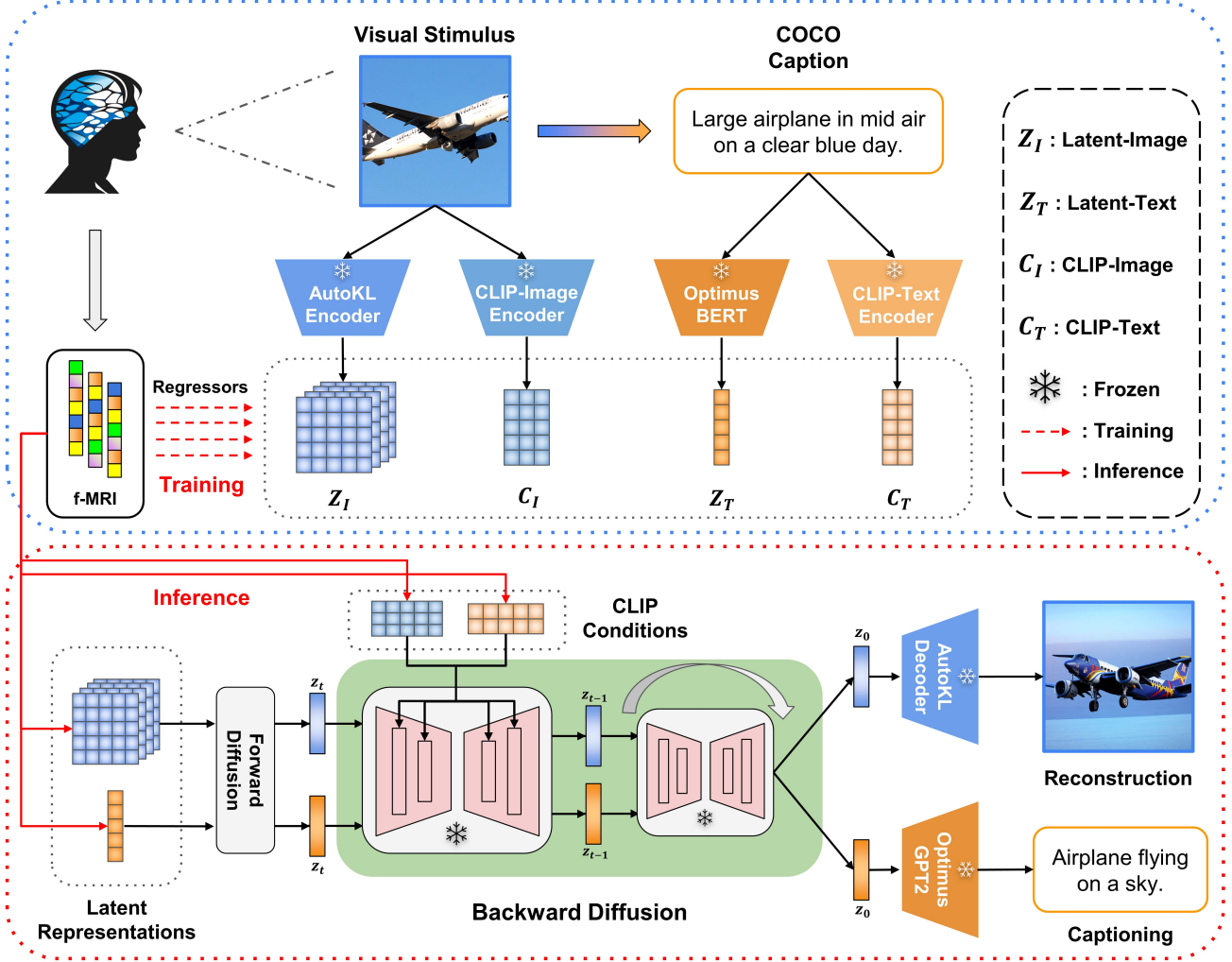


Figure 2. Framework of UniBrain. In the training stage (top), we map fMRI voxels to Latent-Image Z_I , Latent-Text Z_T , CLIP-Image C_I , and CLIP-Text C_T via separated regressors. In the inference stage (bottom), we infer low-level latent (Z_I and Z_T) and high-level CLIP conditions (C_I and C_T) from test fMRI data, which are fed into the pretrained versatile diffusion model for image reconstruction and captioning.

However, DMs that operate in pixel space are computationally expensive. LDMs overcome this limitation by compressing the input using an autoencoder $E(\cdot)$, which is trained on a large-scale image dataset to learn a compressed latent representation z_0 from image x_0 ($z_0 = E(x_0)$). In doing so, the forward diffusion process can be denoted as $z_t = \sqrt{\alpha_t}z_0 + \sqrt{1 - \alpha_t}\epsilon_t$. The reverse diffusion process of LDM is similar to that of DM except that it performs in a latent space with additional conditions. This objective function is defined as below:

$$L_{LDM} = E_{z_0, c, \epsilon \sim \mathcal{N}(0,1), t} [\|\epsilon - \epsilon(z_t, t, \tau_\theta(c))\|^2] \quad (2)$$

where $\tau_\theta(c)$ is the conditioning input for U-Net. The crucial aspect of this procedure lies in its potential to guide

the inverse diffusion process using various conditions (e.g. labels, captions, images and semantic maps). The process of conditioning is accomplished by integrating conditions $\tau_\theta(c)$ within the cross-attention block of the denoising U-Net model. The denoised latent variable derived from the reverse diffusion is passed through the pretrained decoder $D(\cdot)$ to produce a high-quality image.

Versatile Diffusion (VD) [42] is a multi-flow multimodal latent diffusion model capable of producing diverse types of results (e.g. image and text) guided by CLIP features derived from images, text, or image-text pairs. Moreover, VD offers an alternative approach that involves commencing the reverse diffusion process with latent variables acquired from a specific text and image, as opposed to using

entirely random distribution-based initialization. The Versatile Diffusion model utilized in our research was trained on two extensive datasets: Laion2B-en [31] and COYO-700M [4], both of which consist of a substantial number of image-text pairs. The CLIP network employed in VD utilizes the transformer framework (ViT-L/14) and undergoes pretraining via an extensive contrastive task [23].

2.2. Image Reconstruction and Captioning

Based on versatile diffusion, we propose a multi-task multi-modality model termed UniBrain for image reconstruction and captioning from visual-evoked fMRI. The framework of UniBrain is shown in Figure 2. Specifically, following the text-to-text and image-to-image pipelines, we perform a pretrained AutoKL encoder and Optimus BERT [6] encoder on visual stimuli and corresponding COCO [18] captions (random selected from five text annotations) to derive low-level latent representations of image and text (represent as Z_I and Z_T), respectively. Furthermore, the pretrained image and text encoders from CLIP are utilized to derive high-level image and text conditions (represent as C_I and C_T) from visual stimuli and COCO captions, respectively.

In the training state (Figure.2 (top)), we train regressors between i) fMRI and Latent-Image Z_I (4x64x64); ii) fMRI and Latent-Text Z_T (1x768); iii) fMRI and CLIP-Image C_I (257x768); iv) fMRI and CLIP-Text C_T (77x768). Note that all encoders are pretrained on large-scale data and frozen in this work. That is, no training or fine-tuning of complex deep neural networks is needed, we only train four tiny regression models. Each regressor maps fMRI voxels to their corresponding distributions in the training state and infers target distributions of test samples in the testing state with frozen weights (Figure.2 (bottom)).

For image reconstruction, we follow the image-to-image pipeline with multi-modality CLIP conditions (both CLIP-Text and CLIP-Image). First, we infer the low-level image latent representation Z_I from test fMRI and pass through the forward diffusion process, deriving the noisy latent representation z_t at time t . Next, we guide the backward diffusion process by adding the inference high-level CLIP-Text C_T and CLIP-Image C_I conditions in the frozen U-Net. The reconstructed image latent representation z_0 is derived after all diffusion steps and given as input to the pretrained AutoKL decoder to generate the high-resolution image.

For image captioning, we follow the text-to-text pipeline with multimodal CLIP conditions. Likewise, we infer the text latent representation Z_T from test fMRI and guide the backward diffusion with CLIP conditions (C_T and C_I) to reconstruct text latent representation z_0 , which is given as input to the pretrained Optimus GPT2 [24] decoder to generate the descriptive caption for visual stimulus. we found that UniBrain tended to produce repeated sentences in gen-

erated captions, which is also reported in the original paper of VD. Hence, we detect and delete the repeated sentences automatically from generated captions for the final results.

Note that we perform CLIP-Image and CLIP-Text conditions to dual-guide the reverse diffusion process in every diffusion step, where the cross-attention matrices for both conditions are mixed through linear interpolation. We define a mixing rate mix between CLIP-Image and CLIP-Text, which may vary from task to task. When $mix = 0.6$, it means that the relative strength of CLIP-Image is 0.6 and that of CLIP-Text is 0.4.

3. Experiments

3.1. Dataset

We employed the publicly accessible Natural Scenes Dataset (NSD) [1], an extensive 7T fMRI dataset gathered from 8 subjects viewing images from the COCO dataset [18]. Subjects viewed each image for 3 seconds while indicating whether they had encountered the image at any prior juncture during the course of the experiment. In this work, we focused on 4 subjects (Sub-1, Sub-2, Sub-3, and Sub-7) who finished all viewing trials. The training set comprised a total of 8,859 images and 24,980 fMRI trials, with the possibility of up to 3 repetitions per image. Meanwhile, the test set encompassed 982 images and 2,770 fMRI trials. In cases where images had multiple repetitions, the fMRI trials were averaged. Note that the test images remained consistent across all subjects, whereas distinct training images were adopted. For semantic content, we utilized corresponding captions that are randomly selected from five text annotations from the COCO dataset.

We utilized the preprocessed scans from NSD for functional data, with a resolution of 1.8 mm. Our analysis involved employing single-trial beta weights derived from generalized linear models, along with region-of-interest (ROI) data specific to early and higher (ventral) visual regions as supplied by NSD. The ROI comprises the following voxel counts for the respective four subjects: [15724, 14278, 13039, 12682]. To access elaborate fMRI preprocessing procedures and further information, kindly refer to the original paper [1] as well as the NSD website¹.

3.2. Implementation

UniBrain is implemented based on the versatile diffusion model². The regression model performed in UniBrain is Ridge regression, which is a linear regression technique that is used to handle the problem of multicollinearity (high correlation) among the predictor variables in a regression model. In the diffusion process, we use 50 diffusion steps

¹<https://naturalscenesdataset.org>

²<https://github.com/SHI-Labs/Versatile-Diffusion>

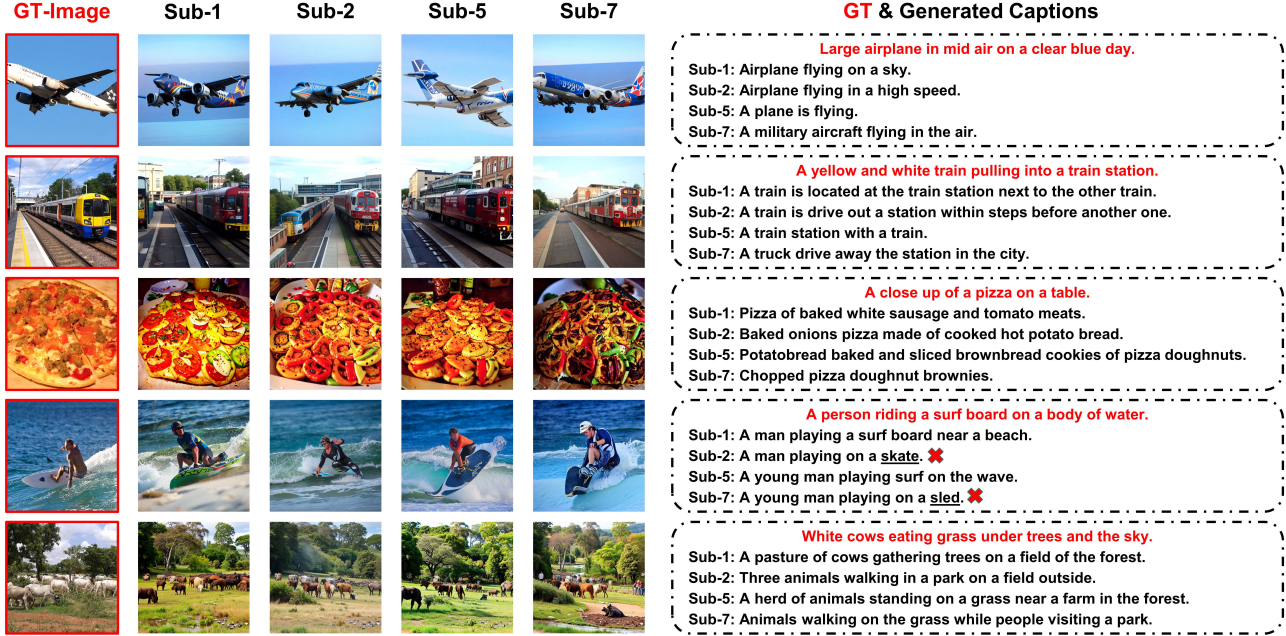


Figure 3. Samples of fMRI-based image reconstruction and captioning from UniBrain. Left: Ground-True images (red box) and generated images from fMRI for all subjects. Right: Ground-True captions (red font) and generated captions from fMRI for all subjects. A red cross next to a font means a mismatch with the original caption in semantics. The presented captions are processed by automatically detecting and removing duplicate sentences from the generated captions.

with a diffusion strength of 0.75 for both text and image latent representations reconstruction. However, the condition mixing rate mix in image reconstruction is different from that in captioning tasks. Specifically, We chose $mix = 0.6$ for image reconstruction and $mix = 0.9$ for image captioning based on the model performance.

3.3. Evaluation Metric

To make quantitative comparisons with current models, we introduce various vision and text evaluation metrics in both low-level and high-level aspects here and report their results in the next session.

3.3.1 Vision Metric

Low-Level: Low-level image features provide basic information about the visual content and structure of the image, measured by: i)**PixCorr**: Pixel-level correlation of reconstructed and ground-truth images; ii)**SSIM**: Structural similarity index [41]; iii)**AlexNet**: AlexNet-2 and AlexNet-5 are the 2-way comparisons of the second (early) and fifth (middle) layers of AlexNet [15], respectively.

High-Level: High-level image features capture semantic information, object relationships, and contextual understanding of the image, measured by: i)**Inception**: A two-way comparison of the last pooling layer of InceptionV3 [36]; ii)**CLIP**: A two-way comparison of the output layer

of the CLIP-Image [23] model; iii)**EffNet**: A distance metric gathered from EfficientNet-B1 [40] model; iv)**SwAV**: A distance metric gathered from SwAV-ResNet50 [5] model.

Regarding the PixCorr and SSIM metrics, we resized the generated images from 512×512 resolution to match the 425×425 resolution of the ground-truth images in the NSD dataset. As for the remaining metrics, the preprocessing of generated images was performed based on the specific input characteristics of each network.

3.3.2 Text Metric

Low-Level: Low-level text features provide basic information about the structure and composition of the text but do not capture the deeper meaning or semantic relationships between words, measured by: i)**Meteor**: The Meteor metric [2] provides a more robust evaluation by considering not only word overlap but also word order, synonymy, and other linguistic aspects that impact translation quality; ii)**Rouge**: Rouge-1 and Rouge-L [16] are specific variants of the Rouge (Recall-Oriented Understudy for Gisting Evaluation) metric that focus on capturing the similarity between the generated and reference summaries.

High-Level: High-level text features are more complex and meaningful representations of text data that capture the context, relationships, and semantics of words and sentences, measured by: i)**CLIP**: A two-way comparison of

Table 1. Compare Results of Image Reconstruction with Current Methods.

Model	Low-Level				High-Level			
	PixCorr \uparrow	SSIM \uparrow	AlexNet-2 \uparrow	AlexNet-5 \uparrow	Inception \uparrow	CLIP \uparrow	EffNet \downarrow	SwAV \downarrow
Mind-Reader [17]	-	-	-	-	0.782	-	-	-
IC-GAN [10]	0.150	0.325	-	-	-	-	0.862	0.465
SD [38]	-	-	0.814	0.815	0.760	0.770	-	-
SD + T [39]	-	-	0.852	0.914	0.858	0.841	-	-
SD+T+G [39]	-	-	0.880	0.929	0.864	0.853	-	-
SD+T+G+D [39]	-	-	0.858	0.921	0.843	0.866	-	-
UniBrain	0.249	0.330	0.929	0.956	0.878	0.923	0.766	0.407

Table 2. Compare Results of Image Captioning with Current Methods.

Subject	Dataset	Low-Level			High-Level
		Meteor \uparrow	Rouge-1 \uparrow	Rouge-L \uparrow	CLIP \uparrow
Ridge-LSTM [37]	GOD [12]	-	-	-	46.4%
PT-LDM [13]	[13]	-	-	0.197	-
CNN-Transformer [43]	[13]	-	-	0.201	-
UniBrain	NSD [1]	0.169	0.245	0.222	85.3%

compared to our model. They recently published a new work [39] to discuss the improvement of the image generation effect after adding components of decoded text (T), GAN images (G), and depth images (D) on the basis of SD. These models are defined as SD+T, SD+T+G, and SD+T+G+D, respectively. However, as shown in Figure 4 (Middle), it seems that adding more components does not always lead to improved outcomes. There are still trade-offs that need to be made based on the generated performance. Nevertheless, these SD variant models are still lacking in low-level details and naturalness when compared to UniBrain.

The Instance-Conditioned GAN (IC-GAN) model [10] produces similar semantics but remains disparities in structural aspects such as shape and texture details, which makes the reconstruction results of IC-GAN less realistic when compared to UniBrain (Figure 4 (Right)). In addition, IC-GAN pretrained on ImageNet may be limited in complex natural scenes with multiple objects.

We compare the image reconstruction results of UniBrain with that of current models quantitatively via the visual metrics described in Section 3.3.1, including low-level and high-level metrics. Note that the metrics reported by previous models vary, but each model has at least one metric compared to ours. As shown in Table 1 (\uparrow means higher is better, and \downarrow means lower is better), UniBrain significantly outperforms all current models in all low-level and high-

level metrics, thus achieving state-of-the-art performance.

4.2. Image Captioning Results

Takada *et al.* [37] transform fMRI data from the GOD [12] dataset into text features via Ridge regression and use the recurrent neural network with long short-term memory (LSTM) for caption generation. Huang *et al.* [13] collect a visual-evoked fMRI dataset themselves and present the PT-LDM model to decode language from fMRI. Specifically, they use a convolutional neural network and a bidirectional GRU neural network to extract features from images and fMRI, which are merged in a GRU neural network to decode sentences. Based on the fMRI dataset collected by Huang *et al.* [13], Zhang *et al.* [43] design a CNN-Transformer hybrid language decoding model to generate descriptive captions for visual stimuli.

Note that UniBrain is the first model that performs image captioning tasks on the NSD dataset and utilizes LDMs for brain-image-text multimodal decoding. Therefore, we only make vague comparisons quantitatively between UniBrain and other previous models via text metrics described in Section 3.3.2. As shown in Table 2, we report the first image-captioning result on the NSD dataset, which performs well on both low-level and high-level metrics.

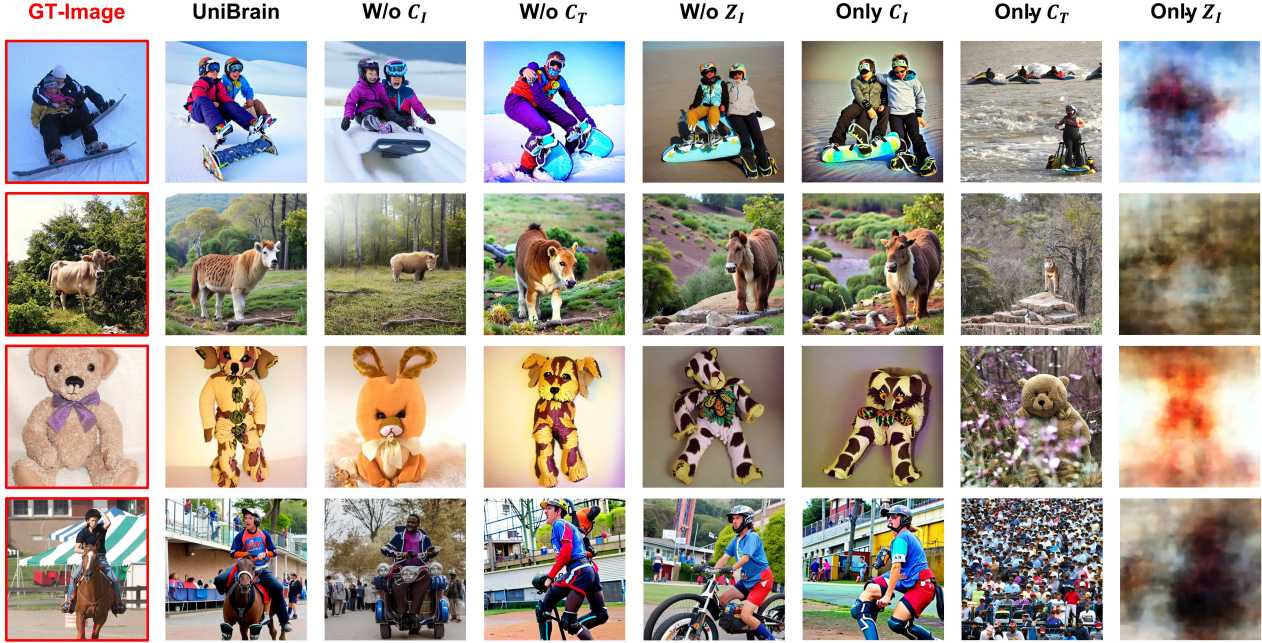


Figure 5. Reconstructed images from UniBrain and its ablation models. ‘W/o Z_I ’ means removing the image latent representation Z_I from the initial UniBrain framework, similar to other ‘W/o’ ablation models. ‘Only Z_I ’ means only feed Z_I to the diffusion process, similar to other ‘Only’ ablation models.

4.3. Ablation Experiments

In order to verify the effectiveness of each component in UniBrain, we conducted ablation experiments on Sub-1 for image reconstruction and captioning, respectively. For image reconstruction, we present qualitative results in Figure 5 and report quantitative measures in Table 3.

As shown in Figure 5, Latent-Image Z_I retains the rough outline and pixels of the original image (‘Only Z_I ’ model). The ‘Only C_I ’ model shows that CLIP-Image features can preserve the global layout and basic semantic information of visual stimuli, such as ‘Two men on snowboards’ (first row), and ‘A cow stands on the mountain’ (second row). The ‘Only C_T ’ model fails in reconstructing images qualitatively, exhibiting that CLIP-Text features can not work alone but brings more high-level semantic details on top of CLIP-Image features (‘Only C_T ’ vs ‘Only C_I ’ vs ‘W/o Z_I ’). UniBrain combines the advantages of each component and finally reconstructs images with both low-level details (pixels and contours) and high-level semantic information (object relationships, and contextual understanding) from fMRI.

Table 3 further validates our conclusions from a quantitative perspective. Specifically, the ‘Only Z_I ’ model achieves the best performance in pixel indicators, and the removal of latent information (‘W/o Z_I ’) makes UniBrain drop sharply in all Low-Level indicators, which proves that Z_I retains most of the low-level features. Furthermore, we noticed

that: i) ‘Only C_I ’ significantly outperforms the ‘Only C_T ’ model in all low-level and high-level metrics; ii) ‘W/o C_I ’ performs worse than ‘W/o C_T ’ in all high-level metrics; iii) ‘W/o C_I ’ is even worse than ‘Only C_I ’ in all high-level metrics; iv) ‘W/o Z_I ’ outperforms ‘Only C_I ’ in all high-level metrics. These results reveal that CLIP-Image retains more basic information about the original image during image reconstruction, and the semantic features extracted by CLIP-Text need to be built on top of this. That is, CLIP-Image pays more attention to the overall semantic information, while CLIP-Text pays more attention to the detailed semantic information. We all know that details need to work better on the whole. Interestingly, though Z_I performs poorly on high-levels matrices, it boost the performance of C_T (‘Only C_T ’ vs ‘W/o C_I ’) and C_I (‘Only C_I ’ vs ‘W/o C_T ’).

Note that, even when combined with C_T and Z_I , as with Takagi *et al.* [38], all quantitative high-level performance of the ‘W/o C_I ’ model is still worse than the ‘Only C_I ’ model. This phenomenon explains why UniBrain is superior to SD [38], since SD ignores the C_I features. The direct comparison between UniBrain and the ‘w/o C_I ’ model more intuitively demonstrates the significant improvement that C_I brings to UniBrain. UniBrain achieves the best in all indicators except pixel indicators (PixCorr and SSIM, UniBrain is the second best), indicating the effectiveness of fusing different components in UniBrain.

Table 3. Ablation results of UniBrain for Sub-1 Image Reconstruction.

Model	Low-Level				High-Level			
	PixCorr \uparrow	SSIM \uparrow	AlexNet-2 \uparrow	AlexNet-5 \uparrow	Inception \uparrow	CLIP \uparrow	EffNet \downarrow	SwAV \downarrow
Only Z_I	0.376	0.419	0.866	0.762	0.547	0.532	0.993	0.674
Only C_T	0.015	0.209	0.633	0.788	0.761	0.837	0.872	0.598
Only C_I	0.089	0.289	0.830	0.926	0.863	0.915	0.800	0.436
W/o Z_I	0.062	0.289	0.833	0.927	0.864	0.927	0.778	0.424
W/o C_T	0.270	0.324	0.943	0.968	0.875	0.914	0.787	0.420
W/o C_I	0.331	0.363	0.913	0.926	0.849	0.869	0.811	0.460
UniBrain	0.299	0.342	0.954	0.969	0.890	0.930	0.757	0.396

Table 4. Ablation results of UniBrain for Sub-1 Image Captioning.

Subject	Low-Level			High-Level
	Meteor \uparrow	Rouge-1 \uparrow	Rouge-L \uparrow	CLIP \uparrow
Only Z_T	0.185	0.262	0.233	77.2%
Only C_T	0.118	0.218	0.208	67.7%
Only C_I	0.128	0.178	0.157	82.8%
W/o Z_T	0.161	0.234	0.209	84.9%
W/o C_T	0.136	0.192	0.169	83.4%
W/o C_I	0.113	0.214	0.205	68.0%
UniBrain	0.170	0.247	0.225	86.1%

For image captioning, we report quantitative measures for UniBrain and its ablation models in Table 4. Text is made up of words, unlike images made up of pixels. Words are inherently semantic, pixels are not. Therefore, text latent has high semantic features. It is worth noting that the high-level metric of the ‘Only Z_T ’ model scores even better than that of the ‘Only C_T ’ model. Interestingly, as in image reconstruction, C_I are more important than C_T features in image captioning, and the gap is more pronounced. This also explains why the mixing ratio $mix = 0.9$ is the best-performed value for image captioning. But even so, the performance of UniBrain has been significantly improved compared to the ‘W/o C_T ’ model. This phenomenon is also the same as that found in image reconstruction. C_T works poorly when it works alone, but it can be used as the performance propellant of C_I (‘Only C_T ’ vs ‘Only C_I ’ vs ‘W/o Z_T ’). The caption generation performance of UniBrain degrades when any component is missing. Except for the optimal performance of the ‘Only Z_T ’ model in low-level indicators, UniBrain achieved the best performance in all indicators compared with other models.



Figure 6. Images reconstructed from synthetic fMRI voxels derived by activating specific regions-of-interests (ROIs). The rows present ROIs that are specified with functional localization experiments (Face-ROI, Word-ROI, Place-ROI, Body-ROI).

4.4. ROI Analysis

Beyond brain decoding, UniBrain has the potential to shed light on the functional characteristics of particular regions-of-interest (ROIs) within the human brain. The interpretation of ROI-optimal images for high-level ROIs defined by function is straightforward, as they typically align with the known category preference of each region. As shown in Figure 6, UniBrain produced various face images from Face-ROI, involving both human and animal faces. Pseudo-words and characters on signs or objects were produced within the Word-ROI except for Sub-7. Regarding the Place-ROI, UniBrain generated realistic interior scene

architectural layouts. In the end, UniBrain reconstructed body parts of humans or animals that are participating in active movements from Body-ROI. Directly visualizing the "optimal" stimulation of a given functional brain region can improve our understanding of how human brain responds to external stimuli.

5. Conclusion

In this work, we propose a multi-task multi-modality model termed UniBrain for image reconstruction and captioning from visual-evoked brain activity measured by fMRI. We delved deeper into the capabilities of LDM in integrating brain, image, and text decoding, facilitating the accomplishment of image reconstruction and captioning tasks within a unified model. This effort allows us to fully analyze how human brain processes and understands external visual stimuli. We compared UniBrain with current models for visual-evoked fMRI-based image reconstruction and captioning respectively. Empirical evaluation demonstrated that UniBrain outperforms other models qualitatively and quantitatively in each task. We made a detailed analysis by combining and contrasting the generated results of images and captions. In addition, we conducted ablation experiments and functional ROI analysis to further exhibit the superiority of UniBrain and provide comprehensive insight for visual-evoked brain decoding. A unified model of multi-task and multi-modality will be closer to the way the brain understands the outside world. We anticipate that this work will serve as a wellspring of inspiration for future investigations.

References

- [1] Emily J Allen, Ghislain St-Yves, Yihan Wu, Jesse L Breedlove, Jacob S Prince, Logan T Dowdle, Matthias Nau, Brad Caron, Franco Pestilli, Ian Charest, et al. A massive 7t fmri dataset to bridge cognitive neuroscience and artificial intelligence. *Nature neuroscience*, 25(1):116–126, 2022. 4, 7
- [2] Satanjeev Banerjee and Alon Lavie. Meteor: An automatic metric for mt evaluation with improved correlation with human judgments. In *Proceedings of the acl workshop on intrinsic and extrinsic evaluation measures for machine translation and/or summarization*, pages 65–72, 2005. 5
- [3] Roman Beliy, Guy Gaziv, Assaf Hoogi, Francesca Strappini, Tal Golan, and Michal Irani. From voxels to pixels and back: Self-supervision in natural-image reconstruction from fmri. *Advances in Neural Information Processing Systems*, 32, 2019. 2
- [4] Minwoo Byeon, Beomhee Park, Haecheon Kim, Sungjun Lee, Woonhyuk Baek, and Saehoon Kim. Coyo-700m: Image-text pair dataset. <https://github.com/kakaobrain/coyo-dataset>, 2022. 4
- [5] Mathilde Caron, Ishan Misra, Julien Mairal, Priya Goyal, Piotr Bojanowski, and Armand Joulin. Unsupervised learning of visual features by contrasting cluster assignments. *Advances in neural information processing systems*, 33:9912–9924, 2020. 5
- [6] Jacob Devlin, Ming-Wei Chang, Kenton Lee, and Kristina Toutanova. Bert: Pre-training of deep bidirectional transformers for language understanding. *arXiv preprint arXiv:1810.04805*, 2018. 4
- [7] Prafulla Dhariwal and Alexander Nichol. Diffusion models beat gans on image synthesis. *Advances in neural information processing systems*, 34:8780–8794, 2021. 2
- [8] Tao Fang, Yu Qi, and Gang Pan. Reconstructing perceptive images from brain activity by shape-semantic gan. *Advances in Neural Information Processing Systems*, 33:13038–13048, 2020. 2
- [9] Guy Gaziv, Roman Beliy, Niv Granot, Assaf Hoogi, Francesca Strappini, Tal Golan, and Michal Irani. Self-supervised natural image reconstruction and large-scale semantic classification from brain activity. *NeuroImage*, 254:119121, 2022. 2
- [10] Zijin Gu, Keith Jamison, Amy Kuceyeski, and Mert Sabuncu. Decoding natural image stimuli from fmri data with a surface-based convolutional network. *arXiv preprint arXiv:2212.02409*, 2022. 2, 7
- [11] Jonathan Ho, Ajay Jain, and Pieter Abbeel. Denoising diffusion probabilistic models. *Advances in neural information processing systems*, 33:6840–6851, 2020. 2
- [12] Tomoyasu Horikawa and Yukiyasu Kamitani. Generic decoding of seen and imagined objects using hierarchical visual features. *Nature communications*, 8(1):15037, 2017. 7
- [13] Wei Huang, Hongmei Yan, Kaiwen Cheng, Chong Wang, Jiyi Li, Yuting Wang, Chen Li, Chaorong Li, Yunhan Li, Zhentao Zuo, et al. A neural decoding algorithm that generates language from visual activity evoked by natural images. *Neural Networks*, 144:90–100, 2021. 2, 7
- [14] Kendrick N Kay, Thomas Naselaris, Ryan J Prenger, and Jack L Gallant. Identifying natural images from human brain activity. *Nature*, 452(7185):352–355, 2008. 2
- [15] Alex Krizhevsky, Ilya Sutskever, and Geoffrey E Hinton. Imagenet classification with deep convolutional neural networks. *Advances in neural information processing systems*, 25, 2012. 5
- [16] Chin-Yew Lin. Rouge: A package for automatic evaluation of summaries. In *Text summarization branches out*, pages 74–81, 2004. 5
- [17] Sikun Lin, Thomas Sprague, and Ambuj K Singh. Mind reader: Reconstructing complex images from brain activities. *Advances in Neural Information Processing Systems*, 35:29624–29636, 2022. 2, 6, 7
- [18] Tsung-Yi Lin, Michael Maire, Serge Belongie, James Hays, Pietro Perona, Deva Ramanan, Piotr Dollár, and C Lawrence Zitnick. Microsoft coco: Common objects in context. In *Computer Vision–ECCV 2014: 13th European Conference, Zurich, Switzerland, September 6–12, 2014, Proceedings, Part V 13*, pages 740–755. Springer, 2014. 4
- [19] Yoichi Miyawaki, Hajime Uchida, Okito Yamashita, Masaaki Sato, Yusuke Morito, Hiroki C Tanabe, Norihiro Sadato, and Yukiyasu Kamitani. Visual image reconstruction from

- human brain activity using a combination of multiscale local image decoders. *Neuron*, 60(5):915–929, 2008. 2
- [20] Milad Mozafari, Leila Reddy, and Rufin VanRullen. Reconstructing natural scenes from fmri patterns using bigbigan. In *2020 International joint conference on neural networks (IJCNN)*, pages 1–8. IEEE, 2020. 2
- [21] Thomas Naselaris, Ryan J Prenger, Kendrick N Kay, Michael Oliver, and Jack L Gallant. Bayesian reconstruction of natural images from human brain activity. *Neuron*, 63(6):902–915, 2009. 2
- [22] Vadim Popov, Ivan Vovk, Vladimir Gogoryan, Tasnima Sadekova, and Mikhail Kudinov. Grad-tts: A diffusion probabilistic model for text-to-speech. In *International Conference on Machine Learning*, pages 8599–8608. PMLR, 2021. 2
- [23] Alec Radford, Jong Wook Kim, Chris Hallacy, Aditya Ramesh, Gabriel Goh, Sandhini Agarwal, Girish Sastry, Amanda Askell, Pamela Mishkin, Jack Clark, et al. Learning transferable visual models from natural language supervision. In *International conference on machine learning*, pages 8748–8763. PMLR, 2021. 4, 5, 6
- [24] Alec Radford, Jeffrey Wu, Rewon Child, David Luan, Dario Amodei, Ilya Sutskever, et al. Language models are unsupervised multitask learners. *OpenAI blog*, 1(8):9, 2019. 4
- [25] Ziqi Ren, Jie Li, Xuetong Xue, Xin Li, Fan Yang, Zhicheng Jiao, and Xinbo Gao. Reconstructing seen image from brain activity by visually-guided cognitive representation and adversarial learning. *NeuroImage*, 228:117602, 2021. 2
- [26] Robin Rombach, Andreas Blattmann, Dominik Lorenz, Patrick Esser, and Björn Ommer. High-resolution image synthesis with latent diffusion models. In *Proceedings of the IEEE/CVF conference on computer vision and pattern recognition*, pages 10684–10695, 2022. 2
- [27] Chitwan Saharia, William Chan, Huiwen Chang, Chris Lee, Jonathan Ho, Tim Salimans, David Fleet, and Mohammad Norouzi. Palette: Image-to-image diffusion models. In *ACM SIGGRAPH 2022 Conference Proceedings*, pages 1–10, 2022. 2
- [28] Chitwan Saharia, William Chan, Saurabh Saxena, Lala Li, Jay Whang, Emily L Denton, Kamyar Ghasemipour, Raphael Gontijo Lopes, Burcu Karagol Ayan, Tim Salimans, et al. Photorealistic text-to-image diffusion models with deep language understanding. *Advances in Neural Information Processing Systems*, 35:36479–36494, 2022. 2
- [29] Chitwan Saharia, Jonathan Ho, William Chan, Tim Salimans, David J Fleet, and Mohammad Norouzi. Image super-resolution via iterative refinement. *IEEE Transactions on Pattern Analysis and Machine Intelligence*, 45(4):4713–4726, 2022. 2
- [30] Hiroshi Sasaki, Chris G Willcocks, and Toby P Breckon. Unit-ddpm: Unpaired image translation with denoising diffusion probabilistic models. *arXiv preprint arXiv:2104.05358*, 2021. 2
- [31] Christoph Schuhmann, Richard Vencu, Romain Beaumont, Robert Kaczmarczyk, Clayton Mullis, Aarush Katta, Theo Coombes, Jenia Jitsev, and Aran Komatsuzaki. Laion-400m: Open dataset of clip-filtered 400 million image-text pairs. *arXiv preprint arXiv:2111.02114*, 2021. 4
- [32] Katja Seeliger, Umut Güçlü, Luca Ambrogioni, Yagmur Güçlütürk, and Marcel AJ van Gerven. Generative adversarial networks for reconstructing natural images from brain activity. *NeuroImage*, 181:775–785, 2018. 2
- [33] Jascha Sohl-Dickstein, Eric Weiss, Niru Maheswaranathan, and Surya Ganguli. Deep unsupervised learning using nonequilibrium thermodynamics. In *International conference on machine learning*, pages 2256–2265. PMLR, 2015. 2
- [34] Yang Song and Stefano Ermon. Generative modeling by estimating gradients of the data distribution. *Advances in neural information processing systems*, 32, 2019. 2
- [35] Yang Song, Jascha Sohl-Dickstein, Diederik P Kingma, Abhishek Kumar, Stefano Ermon, and Ben Poole. Score-based generative modeling through stochastic differential equations. *arXiv preprint arXiv:2011.13456*, 2020. 2
- [36] Christian Szegedy, Vincent Vanhoucke, Sergey Ioffe, Jon Shlens, and Zbigniew Wojna. Rethinking the inception architecture for computer vision. In *Proceedings of the IEEE conference on computer vision and pattern recognition*, pages 2818–2826, 2016. 5
- [37] Saya Takada, Ren Togo, Takahiro Ogawa, and Miki Haseyama. Generation of viewed image captions from human brain activity via unsupervised text latent space. In *2020 IEEE International Conference on Image Processing (ICIP)*, pages 2521–2525. IEEE, 2020. 7
- [38] Yu Takagi and Shinji Nishimoto. High-resolution image reconstruction with latent diffusion models from human brain activity. In *Proceedings of the IEEE/CVF Conference on Computer Vision and Pattern Recognition*, pages 14453–14463, 2023. 2, 6, 7, 8
- [39] Yu Takagi and Shinji Nishimoto. Improving visual image reconstruction from human brain activity using latent diffusion models via multiple decoded inputs. *arXiv preprint arXiv:2306.11536*, 2023. 7
- [40] Mingxing Tan and Quoc Le. Efficientnet: Rethinking model scaling for convolutional neural networks. In *International conference on machine learning*, pages 6105–6114. PMLR, 2019. 5
- [41] Zhou Wang, Alan C Bovik, Hamid R Sheikh, and Eero P Simoncelli. Image quality assessment: from error visibility to structural similarity. *IEEE transactions on image processing*, 13(4):600–612, 2004. 5
- [42] Xingqian Xu, Zhangyang Wang, Eric Zhang, Kai Wang, and Humphrey Shi. Versatile diffusion: Text, images and variations all in one diffusion model. *arXiv preprint arXiv:2211.08332*, 2022. 2, 3
- [43] Jiang Zhang, Chen Li, Ganwanming Liu, Min Min, Chong Wang, Jiyi Li, Yuting Wang, Hongmei Yan, Zhentao Zuo, Wei Huang, et al. A cnn-transformer hybrid approach for decoding visual neural activity into text. *Computer Methods and Programs in Biomedicine*, 214:106586, 2022. 2, 7